

Fabrication and Characterization of Core Shell Fe₃O₄@SiO₂ /P-AM Nanocomposites for Efficient Cu (II) ions Adsorption from Waste Water*Zahra A. Ismail^a, Usama A. Saed^b**^{a,b}Chemical Engineering Department, College of Engineering , AlNahrain University, Baghdad, Iraq.*zahraamerismail@gmail.comusama.a.saed@nahrainuniv.edu.iq

Received:	6/11/2023	Accepted:	19/11/2023	Published:	15/4/2024
------------------	-----------	------------------	------------	-------------------	-----------

Abstract

In this research, poly acrylate-acrylamide (P-AM) was incorporated into an iron (Fe₃O₄@SiO₂) nanocomposite to develop a Fe₃O₄@SiO₂/P-AM adsorption material for Cu (II) ion adsorption. First, Fe₃O₄ was synthesised, then coated with Silica, and ultimately, Fe₃O₄@SiO₂/P-AM was produced using the co-precipitation method. Meanwhile, The aqueous phase dispensability of the Poly acrylate-acrylamide (P-AM) material increases inclusion adsorption efficacy and the adsorption process. The polymer's structural and morphological characteristics were cautiously studied utilising advanced techniques such as XRD, FE-SEM, EDX, TEM, AFM, FTIR, and BET surface area characterization. Pleasantly, the Fe₃O₄@SiO₂/P-AM nanocomposite displayed substantially higher adsorption effectiveness than its component elements, resulting in a remarkable removal rate of about 89.3% during 360 minutes. The adsorption process was fully examined, with four independent factors taken into account: periods of time ranging from 5 to 360 minutes, solution's pH is ranging from 3 to 12, adsorbent dosage ranging from 1 to 3 g/L, and Cu (II) concentration ranging from 25 to 125 mg/L. The best parameters for removing copper metal by adsorption utilising Fe₃O₄@SiO₂/P-AM as adsorbent material were pH 7, 3 g/L dosage of adsorbent, contact time 360 min, and starting Cu (II) ion concentration of 25 mg/L, according to the experimental results. Furthermore, the Langmuir Isotherm was used to analyse and characterise the adsorption process, with regression (R²) of 0.99 indicating the best match to the equilibrium data. According to this definition, the process is mono-layer adsorption on a homogenous adsorbent surface with no contact between the adsorbed molecules. In comparison to other models, the Kinetic analysis reveals that the experimental data matches pseudo-second-order model (R² =0.99). Furthermore, because it is magnetic and stable, it is extremely likely to be employed in practise.

Keywords: Polymeric Nanocomposites, copper ion, adsorption, batch adsorption, Water treatment, Fe₃O₄@SiO₂/P-AM Nanocomposites, and Metal ions.

Introduction

Water contamination by heavy metals that are harmful, such as copper, mercury, lead, chromium, and arsenic is a major global environmental hazard. These heavy metals are very toxic and have been associated to a variety of negative health consequences in humans, including renal disease, respiratory problems, bone abnormalities, cancer, and high blood pressure. The biggest contributors to the release of copper and other heavy metals into the environment are various industrial activities, such as electroplating, smelting, alloy manufacture, pigment production, plastic production, battery manufacturing, mining, and refining [1],[2]. These heavy metals build quickly in organisms and can harm both the environment and human health [3],[4].

Aquatic ecosystem pollution with copper has complex and wide-ranging negative effects. It may get into these ecosystems from a number of different places, including runoff from agriculture, industrial discharges, and weathering of rocks. After being injected, copper stays in these settings for long stretches of time, contaminating food chains and directly endangering human populations [5],[6]. Exposure to copper can impact human health in both positive and negative ways. One of the vital trace elements, copper is involved in many biological processes, including the action of enzymes. Too much copper exposure can be poisonous and have negative health effects. Acute copper poisoning can result in a number of clinical disorders, and in extreme circumstances, even death [7]. Severe neurological abnormalities, anaemia, and liver poisoning have all been linked to prolonged exposure to copper. Long-term exposure to copper dust in work environments has been investigated, and it was discovered that cumulative exposure to respirable copper dust did not negatively impact lung function [8]. Given that exposure to copper nanoparticles has been demonstrated to cause certain pathological alterations in organs as well as an increase in the blood content of ceruloplasmin, it is crucial to take the particle size distribution of copper aerosols into account. In general, the degree, duration, and individual susceptibility of copper exposure all affect health outcomes [9].

Adsorption is a practical and economical way to extract heavy metal ions from wastewater with low concentrations. It has benefits including efficient adsorption, quick absorption, no sludge production, energy economy, and simple operation. For this aim, a variety of adsorbents have been employed in the literature, such as mesoporous silica [10], activated carbon [11], and inexpensive natural lignocellulosic substrates. For highly concentrated wastewater, other methods such as reverse osmosis, chemical treatment, and electrochemical treatments are frequently used; but, in less concentrated circumstances, these methods might be costly. Conversely, adsorption works well with wastewater that has low concentrations and may still maintain a significant amount of adsorption capacity in these situations [12]. Owing to their large surface area and superparamagnetism, magnetic nanoparticles (MNPs), in particular Fe₃O₄, have drawn attention as adsorbents for the heavy metal ions removal from solutions [13]. Fe₃O₄ MNPs, however, have several drawbacks, such as their sensitivity to oxidation and congestion, which can reduce their surface area, recyclable nature, and reactivity[14]. A protective coating layer is frequently applied to improve chemical stability and dispersion in order to get around these challenges [15]. Because of its ease of surface alteration, chemical resilience, and compatibility with biological systems, silica has been acknowledged as an ideal coating option for Fe₃O₄ MNPs [16]. Fe₃O₄@SiO₂ magnetic composite particles have been

shown to be efficient for adsorption in earlier studies, emphasising their quick and reliable adsorption capabilities [17].

Polymers with poly-amines and poly-carboxyl groups have shown good heavy metal ion adsorption performance. Effective adsorption of heavy metal complexes is made possible by the rational microenvironment created via altering a triethylenetetramine (TETA) chain's stretch state in an amine-functionalized porous organic polymer (POP) [18].

In this study, solution dispersion polymerization was used to create a nanocomposite that had more carboxylate and amino groups on its surface. The goal was to methodically examine the composites' capacity for adsorption of Cu (II) ions. The characteristics of the synthesized adsorbent were assessed using XRD, FE-SEM, EDX, FTIR, AFM, TEM, and BET surface area characterization techniques. The study examined the combined effects of solution pH, adsorbent dose, and Cu (II) concentration on the removal efficiency (R%) as the responses. Additionally, various adsorption isotherm models were evaluated, and also the different adsorption kinetic models, such as pseudo-first-order, pseudo-second-order.

2- Experimental Section

2.1 Chemicals

NaOH (LOBA Chemie, India), $\text{FeCl}_3 \cdot 6\text{H}_2\text{O}$ (LOBA Chemie; 10 g) and $\text{FeSO}_4 \cdot 7\text{H}_2\text{O}$ (SCHARLAU, Spain; 10g), ethanol (Alpha Chemika, India), ammonia (30% NH_3 ; Applichem Panreac), Tetraethylorthosilicate (TEOS $\geq 99.0\%$; Fluka), $\text{K}_2\text{S}_2\text{O}_8$, HCl (ReAgent, UK), Acrylic Acid (AA), Aryle Amide (AM).

2.2 Co-precipitation technique for synthesis of Fe_3O_4 nanoparticles

Using a dropper, 500 mL of 1.5 M NaOH was added to the combination of $\text{FeCl}_3 \cdot 6\text{H}_2\text{O}$ and $\text{FeSO}_4 \cdot 7\text{H}_2\text{O}$ at 80°C while stirring continuously. 50 mL of 0.5 M HCl was used to dissolve 5g. After that, the Fe_3O_4 precipitant that was created was gathered using a magnet, repeatedly cleaned in deionized water, and allowed to dry for seven hours at 50°C to get the final form as shown in Fig.1.

2.3 Synthesis of Fe_3O_4 nanoparticles covered with silica

30 mL of pure ethanol (Alpha Chemika, India), 10 mL of deionized water, and 1 mL of ammonia 30% NH_3 were added to Fe_3O_4 nanoparticles in 0.5 g. This concoction was kept for 30 minutes in an ultrasonic tank, and then added Tetraethylorthosilicate TEOS in 2.5 mL stirred for 22 hours. $\text{Fe}_3\text{O}_4 @ \text{SiO}_2$ nanoparticles was dry at ambient temperature.

2.4 Fabrication of $\text{Fe}_3\text{O}_4 @ \text{SiO}_2 / \text{P-AM}$ Composite Material

First of all, sodium hydroxide was employed in a water bath kept at 5°C to create acrylic acid in neutralization degree. Figure.1 shows the process for producing $\text{Fe}_3\text{O}_4 @ \text{SiO}_2 / \text{P-AM}$ is described below. For 30 minutes, 5 g of $\text{Fe}_3\text{O}_4 @ \text{SiO}_2$ was subjected to ultrasound in 100 mL of distill water. The solution was then transferred to a 500- milliliter container containing 25 mL of Acrylic Acid Na solution (containing 10 g of AA), 10 g of AM, and 0.3 g of TEOS. For duration

of fifteen minutes, the container was filled with gas of nitrogen. The container was then filled with twenty milliliters of $K_2S_2O_8$, and the resulting mixture was raised to $55^\circ C$ approximately one and a half hours.

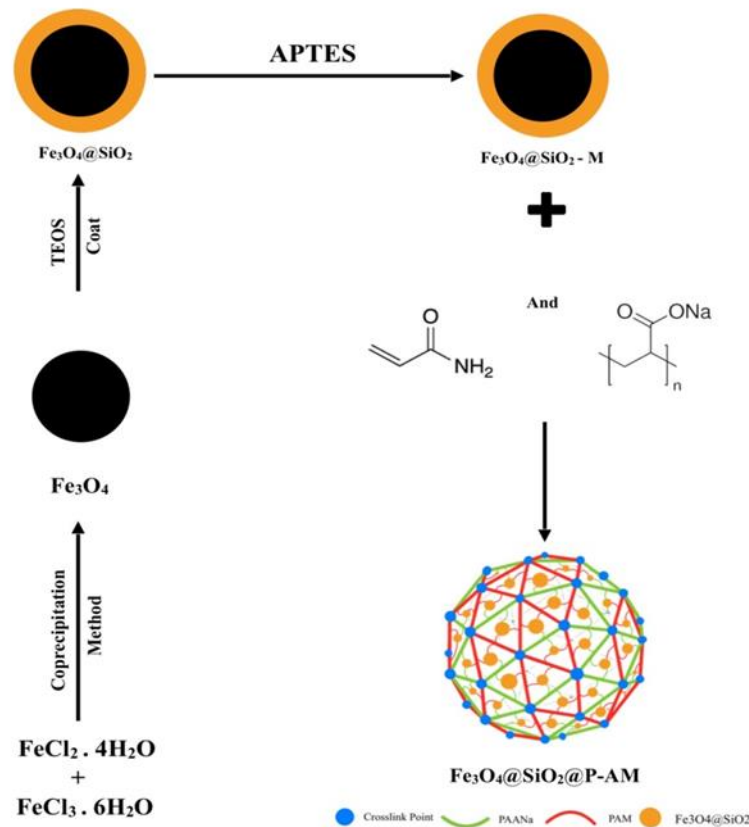


Figure 1. Schematic Synthesis of $Fe_3O_4@SiO_2/P-AM$ Nanocomposites

2.5 Studying Adsorption Processes Experimentally

By dissolving $CuCl_2$ in distilled water and controlling its concentration, a stock solution of $Cu(II)$ was created. Solution's pH was adjusted as necessary with HCl and $NaOH$. Batch tests were run in a shaker set to 60 rpm for 360 minutes at ambient temperature. 100 mL of $Cu(II)$ solution and 0.3 g of adsorbent were used in a standard trial's round-bottom flask to facilitate the adsorption process. The engagement time was changed from 5 to 360 minutes in order to investigate the impact of contact time. By varying the starting Cu^{+2} concentration, which ranged from 25 to 125 ppm, the adsorption isotherm was created in 6 hours. A range of aqueous pH values (3–12) were investigated at room temperature with 0.3 g of catalyst and a starting $Cu(II)$ concentration of 100 ppm. For every test after that, the pH setting that was most appropriate was selected. After

filtering, the concentration of cadmium ions was determined with (AAS) atomic absorption spectrophotometer. The removal rate (R%) and adsorption capacity(q_e) of Cu(II) in mg/g [19], were determined by using equations 1 and 2, respectively. The constants C_0 and C_e in the equations reflect the starting and equilibrium levels of the chemical (in mg/L, respectively). The total solution's volume (in Liters) is represented by V, while the weight of the adsorbent is represented by m (in gram).

$$R (\%) = \frac{C_0 - C_e}{C_0} \times 100\% \quad (1)$$

$$q_e = \frac{(C_0 - C_e)V}{m} \quad (2)$$

3- Result and Discussion

3-Characterization

The crystallographic structure of Fe₃O₄ was evaluated using X-ray diffraction (XRD) analysis after surface modification. The XRD plans of Fe₃O₄, Fe₃O₄ @ SiO₂, and Fe₃O₄ @ SiO₂/ P-AM are shown in Fig. 2. characteristic peaks at $2\theta = 30.4^\circ$, 35.9° , 43.5° , 54.0° , 57.4° , and 63.2° were seen in the pure Fe₃O₄ sample; these peaks corresponded to the crystallographic planes (220), (311), (400), (422), (511), and (440). Similarities were seen in XRD plans of Fe₃O₄ and Fe₃O₄@SiO₂, and all of the recognizable peaks of Fe₃O₄ were preserved in Fe₃O₄@SiO₂, suggesting that the silica coating had no appreciable effect on the crystalline structure of Fe₃O₄ compare with [20]. Interestingly, a strong peak with an intensity of around 103.7 was identified at $2\theta = 35.4^\circ$ in the final results. The P-AM layer in Fe₃O₄@SiO₂/P-AM nanocomposite is responsible for the intensity drop, indicating that the nanocomposite was successfully synthesized.

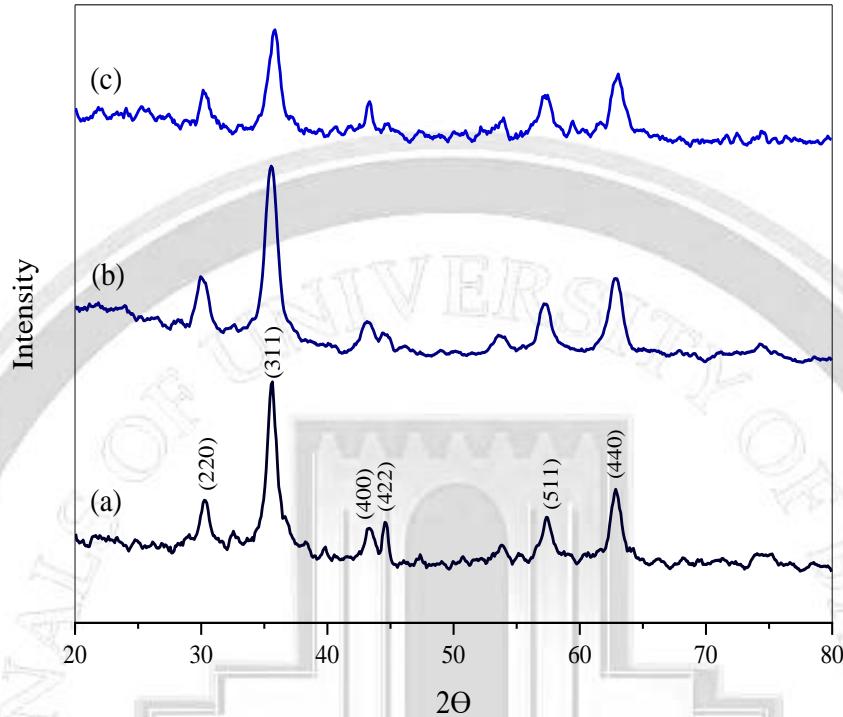


Figure 2. Crystallographic Structure of (a) Fe_3O_4 , (b) $\text{Fe}_3\text{O}_4@SiO_2$, (c) $\text{Fe}_3\text{O}_4@SiO_2/P-AM$

Using FE-SEM (Figure 3a, b, c, and d) to analysis the morphology, the $\text{Fe}_3\text{O}_4@SiO_2/P-AM$ nanoparticle's average size was found to be 14.66 nm. A good platform for heavy metal adsorption is provided by the composite's superfine and plushy structure. The magnetic influence of the nanoparticle is thought to be responsible for the agglomeration effect, since it facilitates the simple separation of the magnetic nano-catalyst compare with [21].

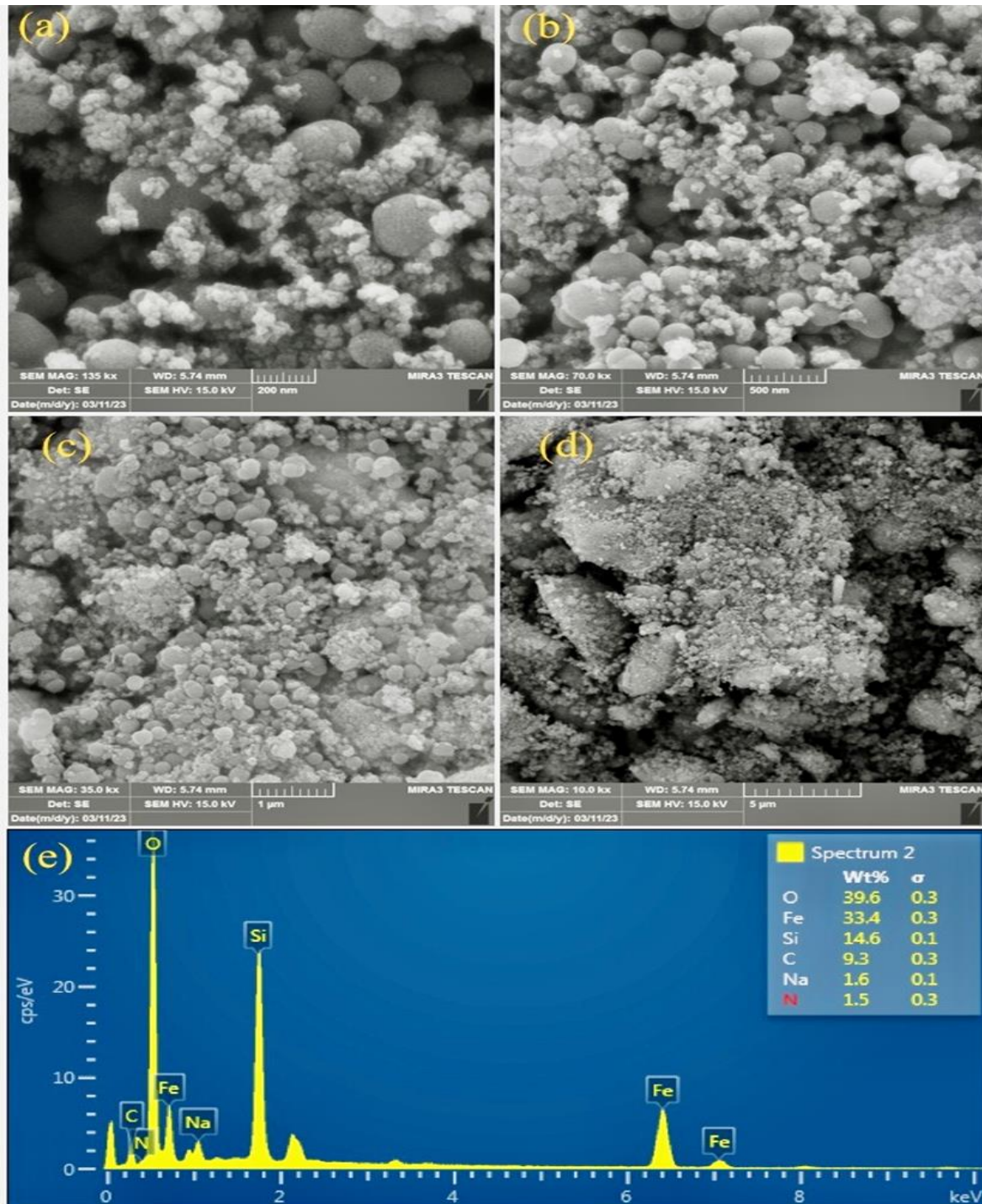


Figure 3. (a, b, c, d) The FE-SEM images for $\text{Fe}_3\text{O}_4@\text{SiO}_2/\text{P-AM}$, (e) The EDX Analysis for $\text{Fe}_3\text{O}_4@\text{SiO}_2/\text{P-AM}$ Nanocomposite.

The purity of Fe₃O₄@SiO₂/P-AM sample was identified using the energy dispersive X-ray analysis (EDX) as shown in Figure 3e. The sample contained the elements O, Fe, Si, C, N, and Na. Furthermore, the sample is incredibly clean since no peaks related to impurities are seen.

To determine the absorbed volume and average surface area, the (BET) surface area analysis test uses N₂ for the adsorption/desorption process. Figure 4. illustrates this. Typical IV isotherms with mesoporous surfaces are represented by the Fe₃O₄@SiO₂/P-AM nanocomposite. Hysteresis loop types found in the highest relative pressure zone indicate the appearance of a meso-porous pore structure in nanocomposite. The pore volume of Fe₃O₄@SiO₂/P-AM is 0.15 cm³/g, the pore size is 11.44 nm, and the specific surface area is 52 m²/g.

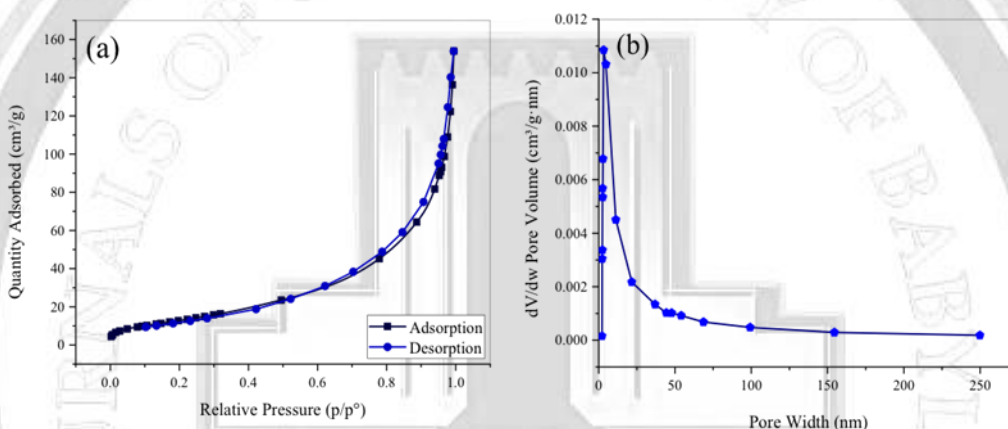


Figure 4. (a) N₂ Adsorption/Desorption and (b) Distribution of Pore Size Curve (BJH method) for Fe₃O₄@SiO₂/P-AM Nanocomposite

The (FT-IR) peak at 571 cm⁻¹ is the typical peak of the Fe–O bond stretching vibration, whereas the wide peak at 1067 cm⁻¹ belongs to the Si–O–Si vibration. This indicates SiO₂ effectively coated Fe₃O₄ particles. Besides, at 805 cm⁻¹ may indicate to N–C vibration for secondary amines, which suggests the successful binding of Fe₃O₄@SiO₂- APTES and the copolymers. While the peak at 1661 cm⁻¹ relates to the telescopic vibration of the carbonyl. C–H bond stretching vibrations are associated with the typical peaks ranging from 2800 to 3300 cm⁻¹. The pre- and post-adsorption spectral lines reveal large and blunt peaks around 2981–3489 cm⁻¹, confirming the existence of association –OH. Figure 5, further depicts the peaks at 1509 cm⁻¹ and 1526 cm⁻¹ are compatible with the symmetric and asymmetrical telescopic peaks of COO⁻. After Cu (II) adsorptions by Fe₃O₄@SiO₂/P-AM, the peaks at 1509 cm⁻¹ and 1526 cm⁻¹ moved to 1490 cm⁻¹ and 1519 cm⁻¹, which is a result of the interaction between Cu and –OH and formation of Cu–OH band.

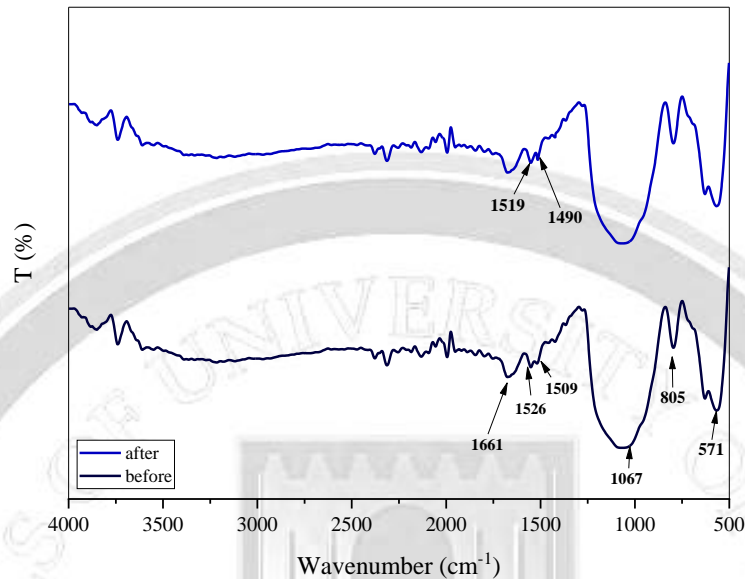


Figure 5. FT-IR for Fe₃O₄@SiO₂/P-AM Nanocomposite Pre- and Post-adsorption.

Using a study with an Atomic Force Microscope (AFM), Fig. 6 shows the different bumpy structure and the nanocomposites particle size distribution, which confirms that the average diameter of the particles is 36.30 nm, and the particle size range is (32-58 nm).

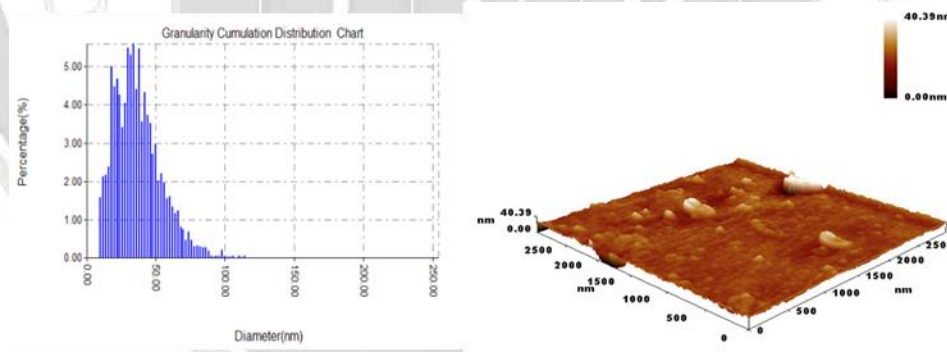


Figure 6. AFM Three Dimensional Image for the Fe₃O₄@SiO₂/P-AM Nanocomposite and the Granularity Accumulation Distribution.

The TEM study as Figure 7. used to examine the morphology of the surface of the nanocomposite. Two unique areas are seen, each with a different concentration of electrons, illustrating how the core-shell structure was formed. The Fe_3O_4 core was located in the middle of the black portion, while the silica shell was near the edge of the grey region. This indicates that SiO_2 covers Fe_3O_4 particles efficiently.

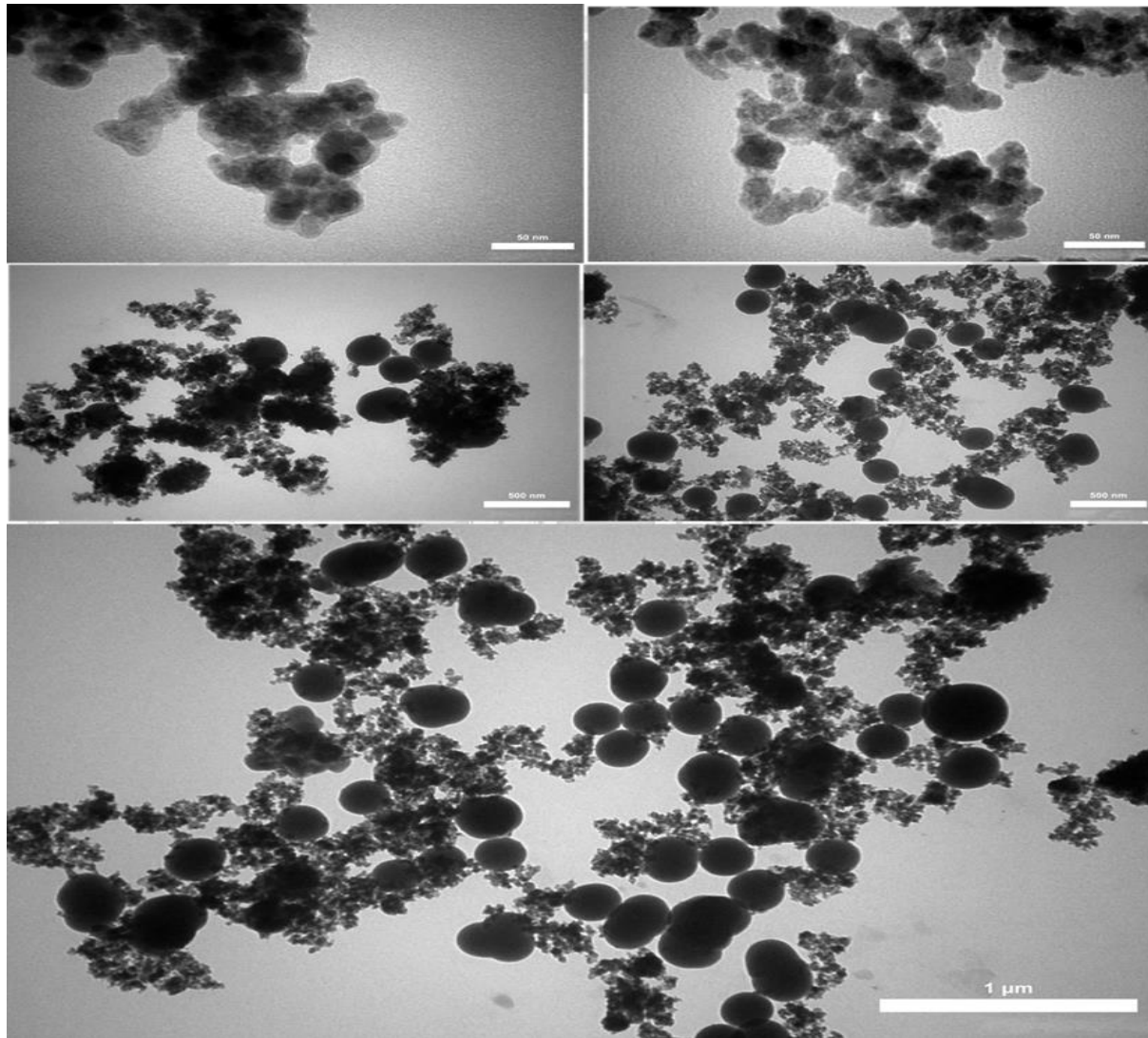


Fig.7.TEM Picture of $\text{Fe}_3\text{O}_4@ \text{SiO}_2/\text{P-AM}$ Nanocomposite.

3.2 Batch Adsorption Experiments

• Effect of contact time: Using $\text{Fe}_3\text{O}_4@\text{SiO}_2/\text{P-AM}$ as catalyst, a variety of trials were conducted. to look at how time affects copper ion adsorption from an aqueous solution as Figure 8. The time-dependent nature of copper ion adsorption was fully investigated using a range of contact times. The aqueous solution was used in 100 ml volumes for the room temperature studies. Using a stock solution, the concentration of the mixture was carefully adjusted to 100 ppm. To speed up the adsorption process and preserve the solution's natural pH, 0.3 g of catalyst was added. No further additives were used. A remarkable maximum removal efficiency of 89.3% for copper ions was attained after 360 minutes. This result highlights the crucial role that time plays in the adsorption process and the $\text{Fe}_3\text{O}_4@\text{SiO}_2/\text{P-AM}$ catalyst's efficaciousness in eliminating copper ions from the aqueous solution.

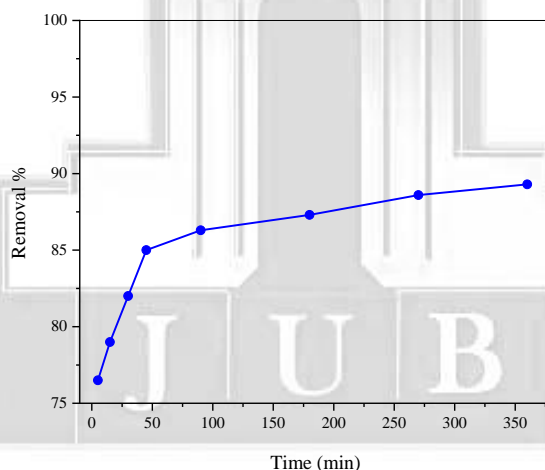


Figure 8. Effect of Contact Time on the Adsorption Removal of $\text{Fe}_3\text{O}_4@\text{SiO}_2/\text{P-AM}$ Nanocomposite

• Effect of pH: When examining the adsorption capabilities of composite materials, the solution's pH is a crucial component. The adsorption performance of $\text{Fe}_3\text{O}_4@\text{SiO}_2/\text{P-AM}$ was examined at pH between 3 and 11 in order to avoid Cu (II) from producing precipitates and to ascertain the ideal pH value for adsorption. The adsorbent's adsorption efficacy steadily rises and eventually stabilizes when the pH value rises. Figure 9. shows that the optimal outcome is achieved when the $\text{Fe}_3\text{O}_4@\text{SiO}_2/\text{P-AM}$ adsorbent is utilized at pH = 7. The electrostatic attraction mechanism between Cu (II) and solution's pH may be the cause of the influence of pH on Cu (II) removal. When the pH is low, say less than 7, the imine group's nitrogen atom

preferentially attaches to protons, leaving Fe₃O₄@SiO₂/P-AM's surface positively charged. This makes it difficult for Cu (II) to adsorb [22].

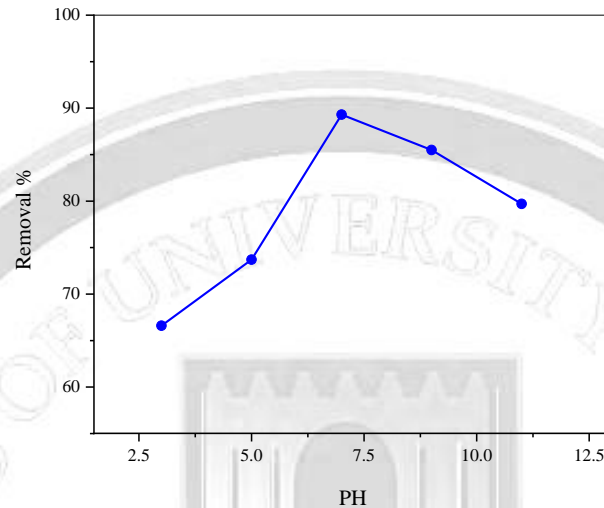


Figure 9. The Influence of pH on Adsorption Removal of Fe₃O₄@SiO₂/P-AM Nanocomposite.

- Impact of metal ion content: Investigating the mechanism of interaction between the adsorbent and the Adsorbate also depends critically on the starting concentration. To examine the impact of the starting ion concentration on the adsorption process, the beginning concentration of Cu (II) was (from 25 mg/ L to 125 mg/ L). As the concentration of contaminant ions rises, the adsorbent may approach equilibrium more quickly at lower concentrations, but the removal efficiency of Fe₃O₄@SiO₂/P-AM for the target heavy metal ions (Cu) is increasing as shown in Figure 10. This is because there are enough vacant active sites that are filled by a restricted number of Adsorbate molecules at a lower concentration [23].

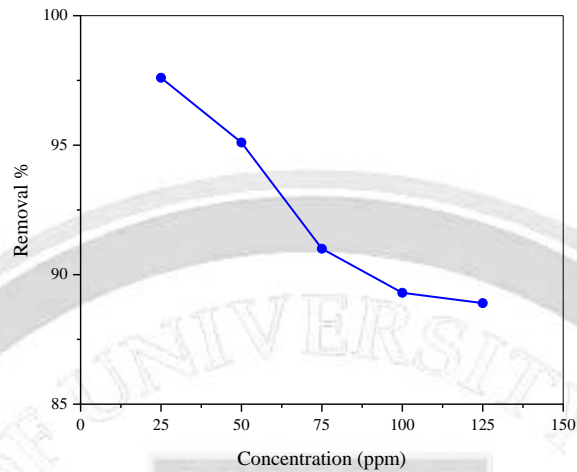


Figure 10. Impact of Concentration on the Adsorption Removal of Fe₃O₄@SiO₂/P-AM Nanocomposite.

• Effect of dose catalyst: Figure 11. demonstrates how a dosage increase significantly increases the pace at which heavy metal ions are removed, while the adsorption capacity steadily declines. This is because the number of active sites given grows with adsorbent quantity, leading to better removal efficiency; nevertheless, dose increments up to a specific concentration do not significantly enhance the removal rate. In contrast, the quantity of free active adsorption sites rises when nearly all of the heavy metals in the aqueous solution are absorbed by the adsorbent, which reduces the adsorbent's adsorption capacity. In addition, Adsorbent aggregation and subsequent reduction in adsorbent adsorption capability can result from high adsorbent concentrations [24]. The effects of the catalyst dose on the rate at which ions of heavy metal removed are examined. There was around 0.3 g of Fe₃O₄@SiO₂/P-AM.

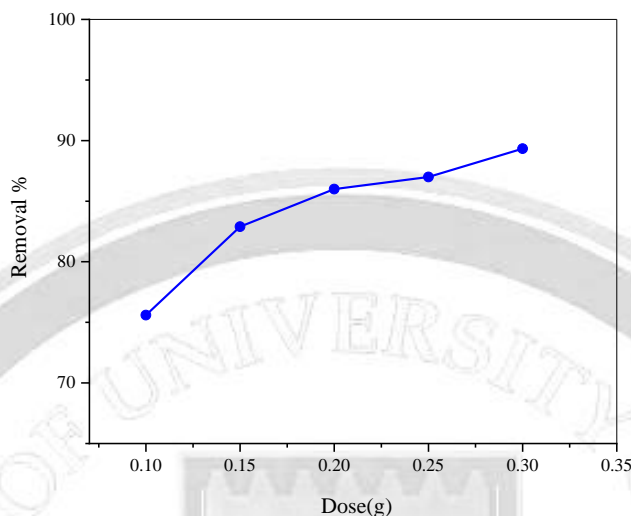


Fig. 11. Effect of Catalyst Dose on the Adsorption Removal of Fe₃O₄@SiO₂/P-AM Nanocomposite.

4- Isotherm and Kinetics Studies

Adsorption isotherm diagrams are frequently used for the investigation of isotherm functions. These figures show how, while maintaining a constant temperature, the amount of adsorbate on the adsorbent and the pressure or concentration relate to one another. The maximal adsorption capacity (q_e) can be ascertained by examining these isotherms. To create an exact equation that captures the observed affects and can be used to design, it is imperative to analyze these isotherms. As Figure 12a shows, three isotherm models; Langmuir, Freundlich, and Temkin models, were employed. Of these models, the Langmuir adsorption isotherm model attracted particular interest since it provided valuable insights into the Fe₃O₄@SiO₂/P-AM sample's adsorption characteristics. [25]. The adsorption equilibrium constant (k_L), which is reported in liters per milligrams, and the maximum quantity of adsorption (q_0), which is measured in milligrams per gram, are important factors in the Langmuir isotherm model. It is possible to determine if the adsorbent surfaces are homogeneous via incorporating data from experiments into the Langmuir model. This allows for the interpretation of the uniformity of adsorption throughout the surface.

The Freundlich isotherm model [26], for Fe₃O₄@SiO₂/P-AM is seen in Figure 12b. The parameters k_f and n in the Freundlich isotherm model stand for the adsorption intensity and capacity, respectively. A smaller fractional value of (n) within the range of 0 to 1 indicates the presence of limited adsorptive forces acting on the surface of the sorbents. Conversely, a value of n greater than one suggests a significant level of adsorption. The versatility of the Freundlich isotherm lies in its applicability to both heterogeneous and homogeneous surfaces, as it portrays the occurrence of multi-layer adsorption.

In Figure 12c, the Temkin isotherm model is presented. According to this model [27], the findings suggest a linear drop in the adsorption heat of all molecules as the surface coverage of the adsorbent increases. This observation implies that the adsorption process is controlled by a steady-state binding energy distribution, eventually reaching the maximum binding energy. When used in this context, the binding constant (kt) stands for the maximal binding energy given in liters per milligrams (L/mg). In addition, the parameter (bt), which is measured in joules per mole (J/mole), is a constant linked to the heat of sorption. The manufactured $\text{Fe}_3\text{O}_4@\text{SiO}_2/\text{P-AM}$ sample exhibits the best degree of fitting for the Langmuir isotherm model ($R^2 = 0.99$), as indicated by the (R^2) values listed in Table 1. Equations (3, 4, and 5) are equations of the Langmuir, Freundlich, and Temkin models, respectively.

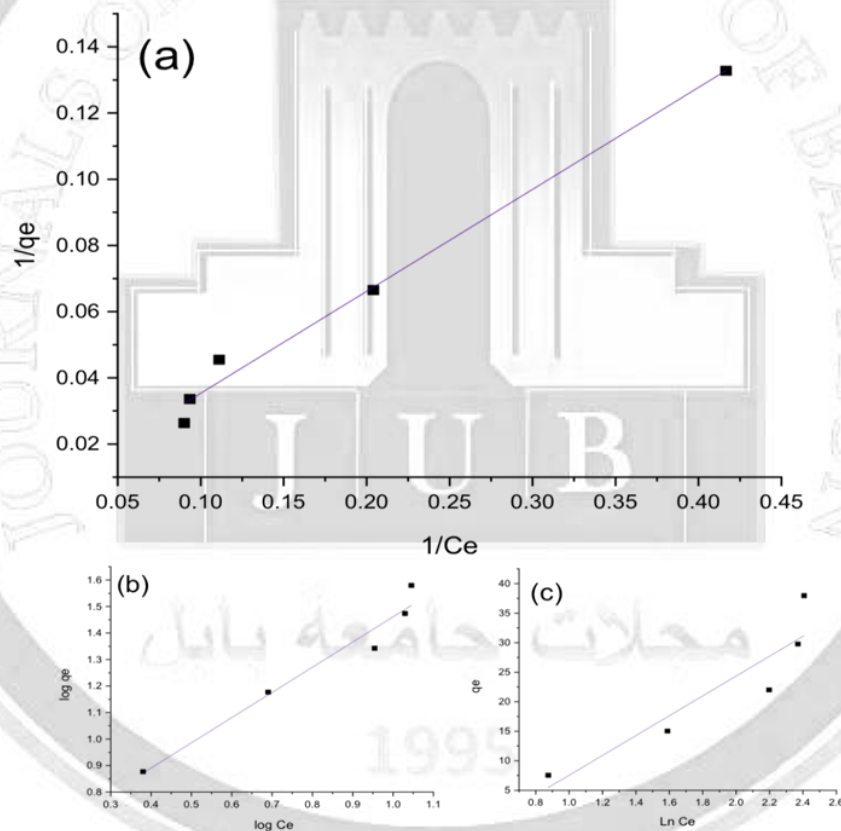


Figure 12. Langmuir Isotherm Model (a), Freundlich Isotherm Model (b), Temkin Isotherm Model (c) of the Prepared $\text{Fe}_3\text{O}_4@\text{SiO}_2/\text{P-AM}$ Nanocomposite.

$$\frac{1}{q_e} = \frac{1}{Q_0 * K_L * C_e} + \frac{1}{Q_0} \quad (3)$$

$$\log q_e = \log K_f + \frac{1}{n} \log C_e \quad (4)$$

$$q_e = \frac{RT}{bt} \ln A + \left(\frac{RT}{bt}\right) \ln C_e \quad (5)$$

Table 1. Isotherm Parameters of the Three Models.

Isotherm model	Parameters	Value
Langmuir	q_0 (mg/g)	0.0296806
$\frac{1}{q_e} = \frac{1}{Q_0 * K_L * C_e} + \frac{1}{Q_0}$	k_L (L/mg)	0.3269199
	R^2	0.99989
Freundlich	K_f (mg/g)	12.352077
$\log q_e = \log K_f + \frac{1}{n} \log C_e$	1/n	0.4801
	R^2	0.94385
Temkin	B_t (J/mol)	10.50124
$q_e = \frac{RT}{bt} \ln Kt + \left(\frac{RT}{bt}\right) \ln C_e$	K_t (L/mg)	3.448632
	R^2	0.73225

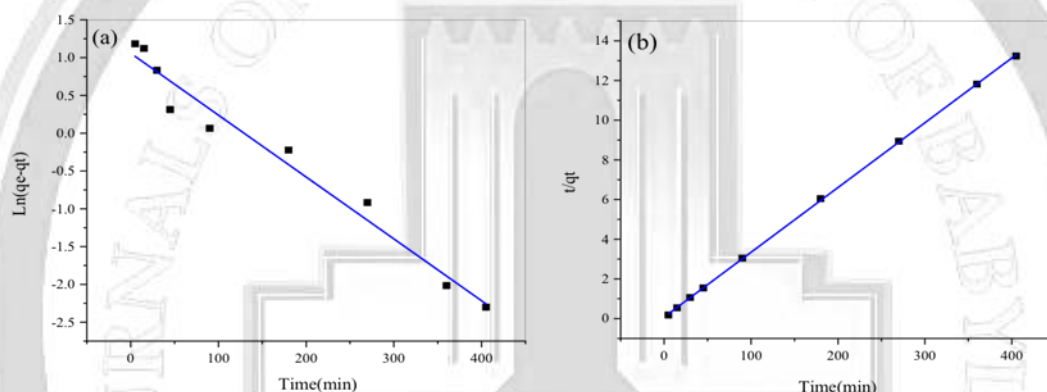
The goal of the experiment was to identify the ideal operating parameters for the batch adsorption process by focusing on the kinetics of copper adsorption on the Fe₃O₄@SiO₂/P-AM adsorbent material. Determining the rate at which the adsorbate stays at the solution border requires an understanding of the adsorption kinetics. In this experiment, two kinetics models were used: the pseudo-first-order and pseudo-second-order models [28]. A number of factors, such as particle size, porosity type, mobility in the solution, and the hydrodynamics of particle interactions in the medium, work together to form and dictate the adsorption rate of a particular molecule. The first and second order models are shown in Fig. 13a and 13b, respectively. Equations (6 and 7) are equations of the kinetics models the pseudo-first-order and pseudo-second-order model, respectively. Where q_t is the amount of chosen compounds adsorbed at time t (mg/g), q_e is the amount of chosen compounds adsorbed at equilibrium (mg/g), and k_1 is the pseudo-first order rate constant (1/min). The rate constant for the second-order equation, denoted as k_2 (g/mg.min), can be observed in the provided data. The table clearly indicates that the Pseudo-second-order model demonstrates the highest level of conformity when applied to Fe₃O₄@SiO₂/P-AM, with an exceptional goodness of fit ($R^2 = 0.99$) ($k_2 = 0.013$ g/mg.min).

$$\ln(q_e - q_t) = \ln q_e - K_1 t \quad (6)$$

$$t/q_e = \frac{1}{K_2 * q_e^2} + \frac{1}{q_e} \quad (7)$$

Table 2. The parameters governing the kinetics of adsorption in the two models.

Adsorption kinetics model	Parameters	Value
Pseudo first order $\ln(q_e - q_t) = \ln q_e - K_1 t$	q_e (mg/g) cal. k_1 (s ⁻¹) R^2	2.87977 -2.02222E-05 0.96817
Pseudo second order $t/q_e = \frac{1}{K_2 * q_e^2} + \frac{1}{q_e}$	q_e (mg/g) cal. k_2 (mg/g.s) R^2	30.6373 0.01352 0.99989

Figure 13. Pseudo-first-order Model (a) and Pseudo-second-order Model (b) of the Prepared Fe₃O₄@SiO₂/P-AM Nanocomposite.

Regeneration Study

To assess the stimulator's long-term efficacy, more research is required. Cu (II) removal rate with Fe₃O₄@SiO₂/P-AM nanocomposite is shown in the data in Figure 14. The Cu (II) species underwent amazing collapse within six reaction cycles. The nanocomposite showed an impressive removal efficacy of 89.3% in the first cycle, but by the sixth cycle, it had decreased to 77.5%. However, the overall effectiveness of the catalyst was hampered by the bulk that was gradually lost during the separation process. This result highlights the excellent regeneration potential of the Fe₃O₄@SiO₂/P-AM composite as a specially formulated adsorbent for Cu (II) removal. The process was carried out through the batch process. In the first cycle, the contaminated water (100 ppm, pH 7, catalyst amount 0.3 g) was mixed with Fe₃O₄@SiO₂/P-AM, and after 360 minutes, The catalyst was extracted using centrifugation, and it was then put to another baker containing polluted water (100 ppm, pH 7, catalyst quantity 0.3 g), and the process was repeated six times.

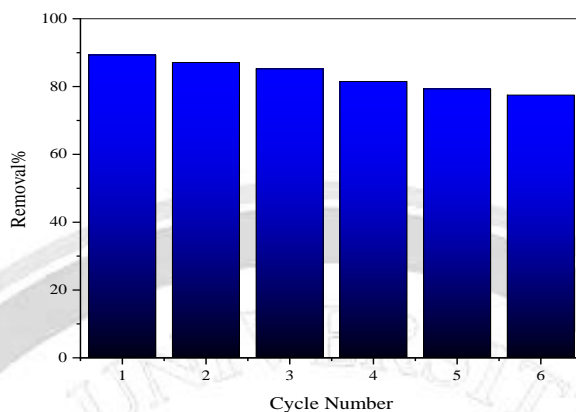


Figure 14 Regeneration Study of Fe₃O₄@SiO₂/P-AM Nanocomposite for Six Cycles at Initial Cu (II) Concentration = 100 ppm, Dose Catalyst = 3 g/L, Reaction Time = 360 min.

Conclusions

Finally, created an efficient Cu (II) ion adsorbent by synthesizing a core-shell amino-functionalized (Fe₃O₄@SiO₂/P-AM) nanocomposite using dual copolymers, acrylic acid (AA) and acrylamide (AM). The polymerization procedure produced discrete active sites on the magnetic core-shell nanomaterial, and the characterization investigations verified the production of the Fe₃O₄ crystal integrated into the silicate structure. Fe₃O₄@SiO₂/P-AM nanocomposites demonstrated impressive Cu (II) adsorption performance, with an initial concentration of 100 ppm and a q_{max} of 220.26 mg/g at pH 7. The dosage of the adsorbent was 3 g/L. It was demonstrated that the Langmuir isotherm model ($R^2 = 0.99$) was the most accurate model for simulating the adsorption process. Additionally, the pseudo-second-order kinetic model ($k_2 = 0.013$ mg/g.s) confirmed that the nanocomposites active sites determine the adsorption rate. According to the mechanism, sorption on the heterogeneous active sites occurs as a rate-dependent step after the first film diffusion stage, which is caused by the attraction of electrostatic charges of the negative charged functional groups on the adsorbent surface. Ultimately, several adsorption-desorption cycles were used to show the reusability of the adsorbent. The results showed material stability, with performance slightly declining from 89.3 to 77.5% after the sixth cycle.

Acknowledgments

This investigation was conducted at al Nahrain University / College of Engineering / Chemical Department, located in Baghdad, Iraq.

References

- [1] A. JAN, S. BANERJEE, and R. CHOUHAN, "HEAVY METAL TOXICITY, BIOACCUMULATION AND OXIDATIVE STRESS IN FRESHWATER FISHES: A SYSTEMATIC REVIEW," UTTAR PRADESH J. Zool., pp. 333–349, 2022.
- [2] S. Soumini, V. Selvaraj, S. Srinivasan, and N. Sreekumar, "Metal pollutants: an environmental hazard," in *Emerging Technologies in Applied and Environmental Microbiology*, Elsevier, 2023, pp. 97–109.
- [3] G. A. Lamas et al., "Contaminant Metals as Cardiovascular Risk Factors: A Scientific Statement From the American Heart Association," *J. Am. Heart Assoc.*, p. e029852, 2023.
- [4] A. Kumari, A. Sinha, and D. B. Singh, "Iron-Based Modified Nanomaterials for the Efficacious Treatment of Cr (VI) Containing Wastewater: A Review," *Persistent Pollut. Water Adv. Treat. Technol.*, pp. 299–331, 2023.
- [5] T. Tomoiye, J. Huang, and N. J. Lehto, "Copper Contamination Affects the Biogeochemical Cycling of Nitrogen in Freshwater Sediment Mesocosms," *Sustainability*, vol. 15, no. 13, p. 9958, 2023.
- [6] Y. Wang, Z. Shu, X. Zeng, W. Kuang, and J. Huang, "Fabrication of O-enriched hypercross-linked polymers and their adsorption of aniline from aqueous solution," *Ind. Eng. Chem. Res.*, vol. 59, no. 25, pp. 11705–11712, 2020.
- [7] A. A. Taylor et al., "Critical review of exposure and effects: implications for setting regulatory health criteria for ingested copper," *Environ. Manage.*, vol. 65, pp. 131–159, 2020.
- [8] L.-M. Haase, T. Birk, A. M. Bachand, and K. A. Mundt, "A health surveillance study of workers employed at a copper smelter—effects of long-term exposure to copper on lung function using spirometric data," *J. Occup. Environ. Med.*, vol. 63, no. 8, pp. e480–e489, 2021.
- [9] A. K. Jaiswal, D. Bhatia, M. Rajesh, and T. Millo, "Analytical aspects and management of copper poisoning-A review," *Indian J. Forensic Community Med.*, vol. 6, no. 3, pp. 110–115, 2019.
- [10] M. T. Kamar, H. Elattar, A. S. Mahmoud, R. W. Peters, and M. K. Mostafa, "A critical review of state-of-the-art technologies for electroplating wastewater treatment," *Int. J. Environ. Anal. Chem.*, pp. 1–34, 2022.
- [11] K. Li et al., "Sustainable application of ZIF-8 for heavy-metal removal in aqueous solutions," *Sustainability*, vol. 13, no. 2, p. 984, 2021.
- [12] P. Asaithambi, M. B. Yesuf, R. Govindarajan, N. M. Hariharan, P. Thangavelu, and E. Alemayehu, "A review of hybrid process development based on electrochemical and advanced oxidation processes for the treatment of industrial wastewater," *Int. J. Chem. Eng.*, vol. 2022, 2022.

- [13] D. Liu et al., "Electrocatalytic reduction of nitrate to ammonia on low-cost manganese-incorporated Co₃O₄ nanotubes," *Appl. Catal. B Environ.*, vol. 324, p. 122293, 2023.
- [14] A. Esmaeilian, D. D. Dionysiou, and K. E. O'Shea, "Incorporating simultaneous effect of initial concentration and sorbent dose into removal prediction model using glyphosate experimental data and theoretical analysis," *Chem. Eng. J.*, vol. 445, p. 136667, 2022.
- [15] Z. Chang et al., "Adsorptive recovery of precious metals from aqueous solution using nanomaterials—A critical review," *Coord. Chem. Rev.*, vol. 445, p. 214072, 2021.
- [16] L. Ouma and M. Onani, "Sequestration of Heavy Metal Pollutants by Fe₃O₄-based Composites," *Inorganic-Organic Compos. Water Wastewater Treat. Vol. 1*, pp. 101–116, 2022.
- [17] S. Venkateswarlu, M. Yoon, and M. J. Kim, "An environmentally benign synthesis of Fe₃O₄ nanoparticles to Fe₃O₄ nanoclusters: Rapid separation and removal of Hg (II) from an aqueous medium," *Chemosphere*, vol. 286, p. 131673, 2022.
- [18] K. Zhao et al., "Hooped amino-group chains in porous organic polymers for enhancing heavy metal ion removal," *ACS Appl. Mater. Interfaces*, vol. 11, no. 47, pp. 44751–44757, 2019.
- [19] J. Sun, Y. Chen, H. Yu, L. Yan, B. Du, and Z. Pei, "Removal of Cu²⁺, Cd²⁺ and Pb²⁺ from aqueous solutions by magnetic alginate microsphere based on Fe₃O₄/MgAl-layered double hydroxide," *J. Colloid Interface Sci.*, vol. 532, pp. 474–484, Dec. 2018, doi: 10.1016/j.jcis.2018.07.132.
- [20] A. Zarei, S. Saedi, and F. Seidi, "Synthesis and application of Fe₃O₄@ SiO₂@ carboxyl-terminated PAMAM dendrimer nanocomposite for heavy metal removal," *J. Inorg. Organomet. Polym. Mater.*, vol. 28, no. 6, pp. 2835–2843, 2018.
- [21] D. Salman et al., "Synthesis, surface modification and characterization of magnetic Fe₃O₄@ SiO₂ core-shell nanoparticles," in *Journal of Physics: Conference Series*, 2021, vol. 1773, no. 1, p. 12039.
- [22] J. Wang, K. Zhang, and L. Zhao, "Sono-assisted synthesis of nanostructured polyaniline for adsorption of aqueous Cr (VI): effect of protonic acids," *Chem. Eng. J.*, vol. 239, pp. 123–131, 2014.
- [23] M. Auta and B. H. Hameed, "Coalesced chitosan activated carbon composite for batch and fixed-bed adsorption of cationic and anionic dyes," *Colloids surfaces B Biointerfaces*, vol. 105, pp. 199–206, 2013.
- [24] L. Fan, C. Luo, Z. Lv, F. Lu, and H. Qiu, "Preparation of magnetic modified chitosan and adsorption of Zn²⁺ from aqueous solutions," *Colloids surfaces B Biointerfaces*, vol. 88, no. 2, pp. 574–581, 2011.
- [25] M. Tuzen, A. Sarı, D. Mendil, O. D. Uluozlu, M. Soylak, and M. Dogan, "Characterization of biosorption process of As (III) on green algae *Ulothrix cylindricum*," *J. Hazard. Mater.*, vol. 165, no. 1–3, pp. 566–572, 2009.

[26] H. B. Senturk, D. Ozdes, A. Gundogdu, C. Duran, and M. Soylak, "Removal of phenol from aqueous solutions by adsorption onto organomodified Tirebolu bentonite: Equilibrium, kinetic and thermodynamic study," J. Hazard. Mater., vol. 172, no. 1, pp. 353–362, 2009.

[27] A. Behnamfard and M. M. Salarirad, "Equilibrium and kinetic studies on free cyanide adsorption from aqueous solution by activated carbon," J. Hazard. Mater., vol. 170, no. 1, pp. 127–133, 2009.

[28] E. D. Revellame, D. L. Fortela, W. Sharp, R. Hernandez, and M. E. Zappi, "Adsorption kinetic modeling using pseudo-first order and pseudo-second order rate laws: A review," Clean. Eng. Technol., vol. 1, p. 100032, 2020.

تصنيع وتوصيف المركبات النانوية ذات القشرة الاساسية $Fe_3O_4@SiO_2/P-AM$ لأمتصاص أيونات النحاس بكفاءة من مياه الصرف الصحي

زهراء عامر اسماعيل اسامة اكرم سعيد

قسم الهندسة الكيميائية، كلية الهندسة، جامعة النهرين، بغداد، العراق.

الخلاصة

في البحث، تم دمج بولي أكريليت-أكريلاميد (P-AM) في مركب نانوي من أكسيد الحديد/السيليكا ($Fe_3O_4@SiO_2$) لتطوير مادة امتصاص $Fe_3O_4@SiO_2/P-AM$ لأمتصاص أيونات النحاس (II). أولاً، تم تصنيع Fe_3O_4 ، ثم تمت إضافة SiO_2 ، وفي النهاية، تم إنتاج $Fe_3O_4@SiO_2/P-AM$ باستخدام طريقة الترسيب المشترك. وفي الوقت نفسه، فإن قابلية الاستغناء عن مادة بولي أكريليت-أكريلاميد (P-AM) في المرحلة المائية تعزز أداء الامتزاز المتضمن وعملية الامتزاز. تمت دراسة الخصائص الهيكلية والمورفولوجية للبوليمر بعناية باستخدام تقنيات متقدمة مثل XRD و FE-SEM و EDX و TEM و AFM و FTIR و BET لتوصيف مساحة السطح. أن المركب النانوي $Fe_3O_4@SiO_2/P-AM$ أظهر فعالية امتصاص أعلى بكثير من العناصر المكونة له، مما أدى إلى معدل إزالة ملحوظ يبلغ حوالي 89.3 % خلال 360 دقيقة. تم فحص عملية الامتزاز بشكل كامل، مع أخذ أربعة عوامل مستقلة في الاعتبار: الفترة الزمنية تتراوح من 5 إلى 360 دقيقة، ودرجة حموضة pH المحلول تتراوح من 3 إلى 12، وجرعة الممتزات تتراوح من 1 إلى 3 جم / لتر، وتركيز النحاس (II) يتراوح من 25 إلى 125 ملغم/لتر. أفضل المعلمات لإزالة معدن النحاس عن طريق الامتزاز باستخدام $Fe_3O_4@SiO_2/P-AM$ كمادة ممتزة هي الرقم الهيدروجيني 7، وجرعة 3 جم / لتر من المادة المازة، والفترة الزمنية 360 دقيقة، وبدء تركيز أيون النحاس (II) بمقدار 25 مجم / لتر. ، وفقاً للنتائج التجريبية. علاوة على ذلك، تم استخدام نموذج Langmuir Isotherm لتحليل وتوصيف عملية الامتزاز، حيث يشير الانحدار (R_2) بمقدار 0.99 إلى أفضل تطابق مع بيانات التوازن. وفقاً لهذا التعريف، فإن العملية عبارة عن امتزاز أحادي الطبقة على سطح ممتز متجانس مع عدم وجود اتصال بين الجزيئات الممتزة. بالمقارنة مع النماذج الأخرى، يشير التحليل الحركي إلى أن البيانات التجريبية تتطابق بشكل جيد مع نموذج الدرجة الثانية الزائفة ($R_2 = 0.99$). علاوة على ذلك، نظراً لكونه مغناطيسياً ومستقرًا، فمن المحتمل جداً استخدامه في الممارسة العملية.

الكلمات الدالة: المركبات النانوية البوليمرية، أيون النحاس، الامتزاز، معالجة المياه، $Fe_3O_4@SiO_2-M/P-AM$ ، المركبات النانوية.